Time scales in fragmentation

A. Strachan and C. O. Dorso
Departamento de Física, Facultad de Ciencias Exactas y Naturales, Universidad de Buenos Aires, Pabellon I, Ciudad Universitaria, Nuñez 1428, Buenos Aires, Argentina
(Received 9 September 1996)

The problem of fragmentation of excited finite systems is explored in the frame of classical molecular dynamics experiments of two-dimensional Lennard-Jones drops. The main objective of this work is to get information about the relative value of the relevant characteristic time scales (CTS) for this kind of process. We investigate the CTS for fragment formation, the stabilization of the radial flux, and the internal ''temperature.'' It is found that the asymptotic fragments are realized early in phase space, when the system is still dense, by the time the radial flux attains its asymptotic value. It is also shown that the temperature of the system during the breakup is quite homogenous with respect to the expected profile if local thermal equilibration takes place. Special emphasis is put on the investigation of the time scale of stabilization of the statistical properties of the mass spectrum, which is related to the kind of information carried by the asymptotic fragments. [S0556-2813(97)04301-X]

PACS number(s): 25.70.Pq, 02.70.Ns, 24.10.Pa

I. INTRODUCTION

Despite the great efforts done in order to study the mechanisms which lead an excited system of nucleons to break up in several intermediate-mass fragments, and the possible connection of this process with a liquid-gas transition, several questions remain unanswered. It is not well known when, how, and which density fluctuations start to develop in the expanding system of nucleons, during the early stages of the process, and become fragments in a later stage. In order to understand why the system becomes unstable with respect to some density fluctuations it is mandatory to determine its most relevant properties during the whole process and to follow in time the development of the density fluctuations which lead to the breakup. The phenomenon of fragmentation is not a specific property of nuclear systems but it is a common feature of many different systems, for example: pressurized fluids flowing through nozzles, rock explosions, protein decay through elongation, etc. All these processes share the lack of knowledge about the dynamics of fragment formation.

In nuclear physics many models have been devised to study the behavior of expanding finite nuclear systems. They can be roughly classified in the three following categories: (1) the ones based on the calculation of the evolution of the one body density function (LV [1], BUU [2]), (2) thermodynamical models, which assume some degree of thermal equilibrium, and that have been developed in the framework of microcanonical [3], canonical [4], and grand canonical [5] ensembles. Finally (3) microscopic dynamical models which contain all the microscopic information at all times, these models have the appealing feature that they bring the possibility of analyzing many body correlations at all times. Amongst this last category we can mention those which are purely classical [6], quasiclassical [7], and semiclassical [8].

Only recently a cluster definition and its recognition algorithm (early cluster recognition algorithm ECRA) has been proposed [9] which allows the analysis of the fragmentation process at all times. In this model the most bound density fluctuation in phase space (MBDF) is studied as a function of time. It has been applied to different molecular dynamics experiments [10–12] and it has been found, in all of them, that the MBDF becomes stable very early in the evolution, when the system is still dense, and that this density fluctuation turn out to be the asymptotic fragments, when it spreads in space due to the expansion.

Regarding the breakup mechanism many authors, based on Fisher's semiphenomenological drop model [13], have related power law behavior of the asymptotic mass spectra in multifragmentation to the disassembly of the system of nucleons at the density and temperature of the critical point. Fisher's model predicts that the mass distribution should be a power law multiplied by an exponential whose argument goes to zero at the critical point. This kind of behavior is indeed observed in different experiments, but it has been shown that the times involved in multifragmentation are far too short to relate the breakup to equilibrium processes like spinodal decomposition or nucleation [12].

Since nuclear matter is a Fermi system an appropriate model should be quantum mechanical in nature, unfortunately such a description is not feasible if one wishes to keep n-body correlations. In our calculations we will try to keep things as simple as possible, so we choose to simulate the behavior of excited finite system via a system of classical Lennard-Jones (L-J) particles, which has an equation of state (EOS) in many respects similar to the one expected for nuclear matter and exhibits liquid-gas phase transition [14]. This model has the important advantage that it has been extensively studied both for finite and infinite systems and has also been applied to the analysis of nuclear collisions [14].

In this communication we focus our analysis on the study of the characteristic time scales (CTS) related to the stabilization of different collective and intrinsic degrees of freedom, as well as cluster formation. As a by-product we will obtain new information about the validity of thermodynamical models and suggestions for their improvement. We also address the problem of which kind of information is contained in the asymptotic mass spectra. We do this by analyz-

ing the stage of the evolution at which the statistical properties of the MBDF spectra is statistically equivalent to the asymptotic mass spectra.

The paper is organized as follows. In Sec. II we describe the model, tools, and CTS used in this work and in Sec. III we present the results of the analysis of the mass spectra of our numerical simulations. In Sec. IV we analyze the time dependence of the radial flux and temperature and in Sec. V we discuss the early cluster formation model. Finally conclusions are presented in Sec. VI.

II. NUMERICAL EXPERIMENTS AND TIME SCALES

As mentioned in the Introduction we simulate nuclear multifragmentation via a classical system of Lennard-Jones particles in two dimensions. The two body interaction potential is taken as

$$V(r)=4\epsilon\left[\left(\frac{\sigma}{r}\right)^{12}-\left(\frac{\sigma}{r}\right)^{6}-\left(\frac{\sigma}{r_c}\right)^{12}+\left(\frac{\sigma}{r_c}\right)^{6}\right],$$

where r_c is the cutoff radius (the potential is taken equal to zero for $r>r_c$). In this calculations we took $r_c=3\sigma$. Energy and distance are measured in units of the potential well (ϵ) and the distance in which the potential changes sign (σ) respectively. The unit of time used is $t_0=\sqrt{\sigma^2/48\epsilon}$. Although it is well known that such a potential presents a too steep repulsive part, i.e., hard equation of state, we use it because the properties of such a system are very well known. In this sense our calculations are mainly pedagogical (for a study on the properties of the L-J potential with respect to the nuclear problem see [14]).

Our work is based on the study of numerical simulations of the time evolution of excited finite two dimensional Lennard-Jones drops of $N=100$ particles, whose initial configurations were obtained by cutting a circular drop from a thermalized periodic system of $N=225$ Lennard-Jones particles, per cell, with periodic boundary conditions. The ground state energy, ϵ_0, of this system of 100 L-J particles was calculated from an almost circular system cut out from a triangular lattice. The distance between nearest neighbors was taken as that distance at which $V(r)$ attains its minimum value ($r_{\min}\sim 1.12\sigma$). We got the result $\epsilon_0\simeq -2.8\epsilon$.

We performed explosions of $N=100$ particles, two-dimensional drops built according to the method described in the previous section. We studied a rather broad range of total energies ranging form $E=-1.15$ to $E=1.8$, which means initial temperature in the range: $1\epsilon-4\epsilon$ for a fixed initial density $\rho=0.75\sigma^{-2}$. This means that our drops are all compressed and heated. This can be seen from Fig. 1 in which we show the metastability curve for an infinite two-dimensional L-J system (full line) [15]. We also show the one corresponding to a periodic system in which each cell is populated with exactly 100 L-J particles (full circles) which we obtained studying the behavior of the specific heat at constant volume C_V with temperature [12]. Noticeable finite size effects are evident. This finite size effects are of the kind usually referred to as bulk effects because they are related to the inhibition of density fluctuations with wavelengths larger than the cell size [12]. The corresponding spinodal lines lie inside the metastability curve. It is worth mentioning at this point that the effect due to free boundaries have not been included in this calculation of the EOS (see for example [16]).

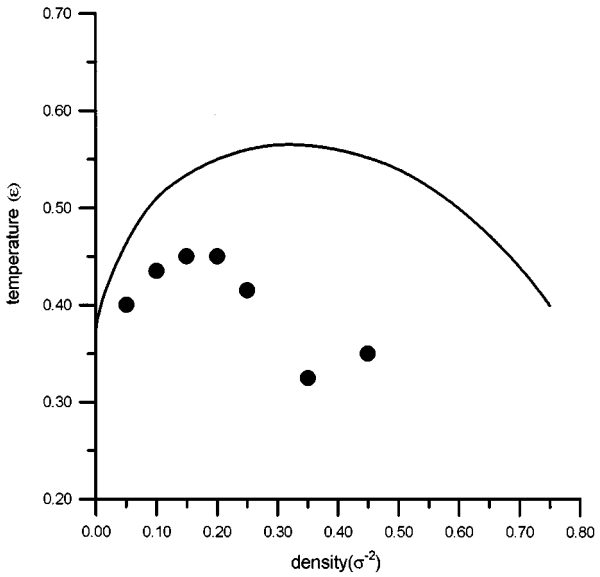

FIG. 1. Metastability curve, in the $T-\rho$ plane, for the infinite two-dimensional Lennard-Jones system (full line) and metastability curve for the $N=100$ periodic Lennard-Jones system (circles).

As stated in the Introduction, we studied, what we consider to be some of the most relevant quantities of the expanding system, as a function of time. One of these quantities is the collective expansion or radial flux. In order to study the mean radial velocity as a function of position we divided our system in ten concentric circular rings and studied the time behavior of the mean radial velocity in each of the regions. The ith region is the area between two concentric circles, centered in the center of mass of the system, of radius $r_1=(i-1)r_{\max}/10$ and $r_1=ir_{\max}/10$, where $r_{\max}$ is the distance of the outermost particle from the center of mass of the system. The mean radial velocity of the ith region is defined as

$$v_{\mathrm{rad}}^{(i)}(t)=\left\langle\left\langle\frac{\mathbf{v}_j(t)\cdot\mathbf{r}_j(t)}{|\mathbf{r}_j(t)|}\right\rangle_i\right\rangle_e,$$

where $\mathbf{r}_j$ and $\mathbf{v}_j$ stand for the position and velocity of the particle j, the symbol $\langle\rangle_i$ represents average over particles which belong to the ith region for a given simulation, $\langle\rangle_e$ denotes the average over the ensemble of simulations performed at given initial conditions.

Another important quantity is the ''temperature'' of each of the circular sectors which we define as the velocity fluctuations around the collective mean radial velocity:

$$T^{(i)}(t)=\left\langle\left\langle\frac{1}{2}m\left(\mathbf{v}_j(t)-\frac{v_{\mathrm{rad}}^{i}(t)\cdot\mathbf{r}_j(t)}{|\mathbf{r}_j(t)|}\right)^2\right\rangle_i\right\rangle_e.$$

These two magnitudes will help us analyze the degree of equilibrium of the system during its evolution.

In order to study the role played by interparticle collisions in the different stages of the multifragmentation process, we found it convenient to define the collision rate at time t_n as

$$C(t_n)=\sum_{i=1}^{N} |\mathbf{v}_i(t_{n+1})-\mathbf{v}_i(t_n)|,$$

where $t_n=nt_{\rm int}$, being $t_{\rm int}$ the time step that we used for the integration of the equations of motion. We took $t_{\rm int}=0.0001t_0$ which guaranteed proper conservation of energy and total momentum.

In this work we investigate the relationship among the time evolution of the radial flux and temperature of the different regions, collision rate, and cluster formation. In order to relate the process of flux formation and possible ''temperature'' equilibration with fragment formation we need to select a fragment definition. In this work we use the following ones.

(i) The simplest cluster definition is based on the two-particle correlations in configuration space: a particle i belongs to a cluster C if and only if there is another particle j which also belongs to cluster C and $|\mathbf{r}_i-\mathbf{r}_j|\leqslant r_{\rm cl}$, where r_{cl} is a parameter called clusterization radius. This cluster definition is valid in the later stages of the process but it gives no information about the early stages of the multifragmentation. This method is known as minimum spanning tree (MST) or configurational. In our calculations we took $r_{cl}=3\sigma$.

(ii) Following Ref. [9] clusters are defined by the most bound partition of the system, i.e., the partition (defined by the set of clusters $\{C_i\}$) which minimizes the sum of the energies of each fragment:

$$E_{\{C_i\}}=\sum_i \left[\sum_{j\in C_i} K_j^{\rm c.m.}+\sum_{j,k\in C_i} V_{j,k}\right],$$

where the first sum is over the clusters of the partition, and $K_j^{\rm c.m.}$ is the kinetic energy of particle j measured in the center of mass frame of the cluster which contains particle j. The algorithm developed to achieve this goal is known as ''early cluster recognition algorithm'' (ECRA) [9]. The partition obtained using this last approach will be called hereafter most bound density fluctuation (MBDF), and we will denote the constituent clusters as fragments only in the low density regime, when the ECRA and MST clusters coincide.

In order to study the possible relation between the most relevant processes like radial flux formation, cluster formation, etc., we found it useful to define the following characteristic time scales (CTS).

$\tau_{\rm flux}$ is the CTS for the stabilization of the collective expansion degree of freedom, usually referred to as radial flux.

$\tau_{\rm temp}$ is the CTS for stabilization of the intrinsic effective ''temperature'' of each circular sector. We are defining just one time because, as will be shown in the next section, all circular sectors thermally stabilize at approximately the same time for each initial excitation energy

$\tau_{\rm coll}$ is the CTS for stabilization of the collision rate.

$\tau_{\rm ecra}$ is the CTS for the formation of the clusters according to the ECRA fragment recognition formalism. The ECRA algorithm provides information of the most bound partition at any time. The resulting fragment spectra reaches stability far earlier than the MST one and reflects the complicated collisional evolution of the system in its early stages. In this way, $\tau_{\rm ecra}$ will be given by the average time at which the fragment spectra becomes stable.

$\tau_{\rm mst}$ is the CTS for the formation of the clusters according to the standard MST approach, i.e., the typical time at which fragments are ammenable to experimental recognition.

From the relation among the above defined CTS we will get a more complete insight of the fragmentation process.

III. PROPERTIES OF THE MASS SPECTRA

In Fig. 2 we show the asymptotic mass spectra for six different energies ranging from $E=1.8\epsilon$ to $E=-0.8\epsilon$ (see figure caption for details). It can be seen that for the higher energies the mass distributions show rapid, exponential, decay with fragment mass and as we move to smaller energies a broader mass spectra is obtained. For energies $E=-1\epsilon$ and $E=-1.15\epsilon$ a transition to U shaped spectra appears. We want to mention at this point that asymptotic mass spectra are those obtained according to the ECRA algorithm at the end of the evolution ($t_{\rm max}$) of the expanding system. In most cases the results from MST recognition method at $t_{\rm max}$ are equivalent to ECRA results at that time. This is not true if the evolutions are not long enough for the system to reach its true asymptotic state.

As mentioned above, one of our main objectives in this work is the study of the time scales related to fragment formation, i.e., we want to know the time at which the asymptotic fragments are already formed and the state of the system at that moment. We performed a cluster analysis of our explosions using both the MST and ECRA methods. In Fig. 3 we show the mass multiplicity spectra for $E=-0.3\epsilon$ for different times, namely $40t_0$, $80t_0$, and $200t_0$, using the MST algorithm (left part of the figure) and ECRA algorithm (right part). It can be clearly seen that for time $40t_0$ the system is still dense and a simple configurational analysis gives no information about the asymptotic behavior, nor does it at time $80t_0$, but the ECRA spectrum is already very similar to the asymptotic one. In Fig. 4 we show again the mass spectra at times $40t_0$, $80t_0$, and $200t_0$ for both algorithms but for $E=-0.8\epsilon$. In Figs. 5(a), 5(b), and 5(c) we show the asymptotic spectra (diamonds) and the ECRA result for time $10t_0$ (squares) for energies $E=-0.15\epsilon$, 0.3ϵ, and 0.8ϵ, respectively. In Fig. 5(c) we also show, for comparison, the MST mass distribution for time $10t_0$ (full circles). From Figs. 3–5 it can be seen that the ECRA model is able to find the asymptotic fragments at very short times when the system is still dense. This result has been found for a variety of molecular dynamics experiments [12,11].

So far we have been comparing mass spectra at different times by simply looking at their shapes; in order to have a quantitative measure of the similarity of two mass distributions one can calculate the probability that the two different spectra come from the same distribution function. This problem can be solved calculating the χ_b^2 statistics for binned data [17]:

$$\chi_b^2=\sum_i \frac{[n_i(t_a)-n_i(t_b)]^2}{[n_i(t_a)+n_i(t_b)]},$$

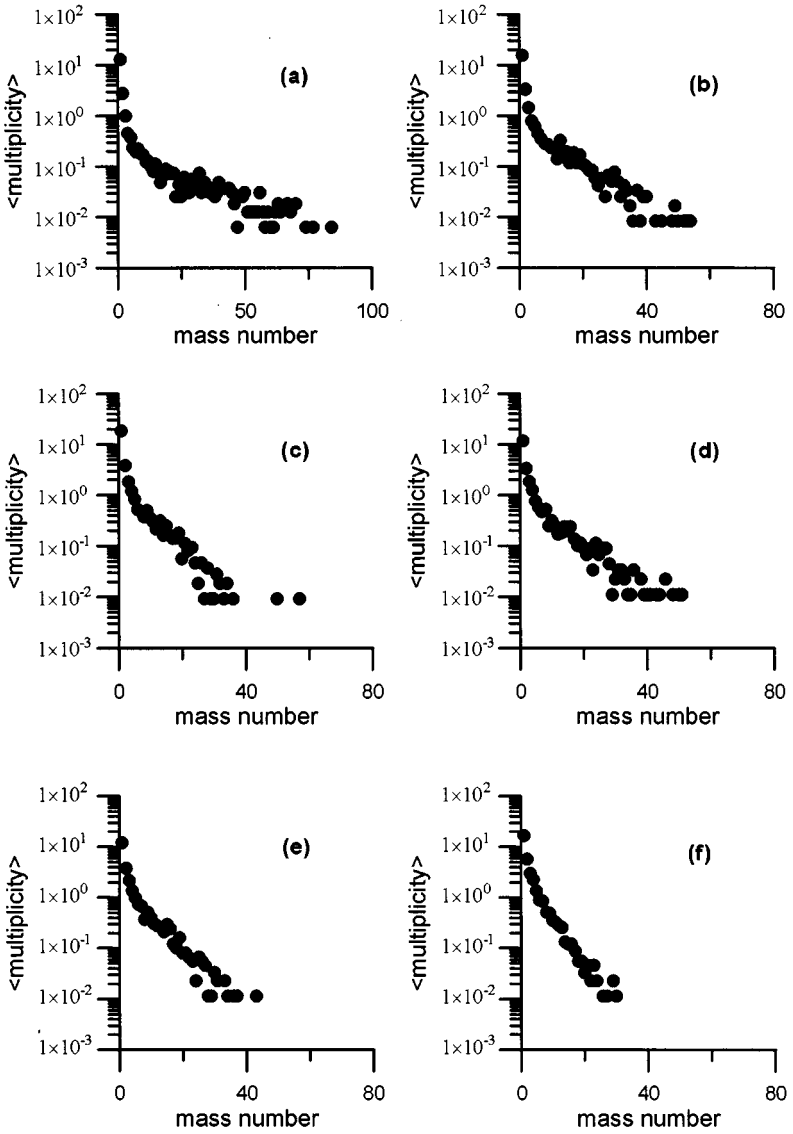

FIG. 2. Asymptotic mass spectra, for energies: (a) $E=-0.8\epsilon$, (b) $E=-0.55\epsilon$, (c) $E=-0.3\epsilon$, (d) $E=-0.015\epsilon$, (e) $E=0.8\epsilon$, and (f) $E=1.8\epsilon$.

where $n_i(t)$ denotes the number of fragments in bin i and the sum runs over a fixed mass range. To have an order of magnitude for the value of χ_b^2 denoting equivalence we have studied this magnitude when different mass spectra are generated from the same probability density distribution function. For this purpose we have generated sets of 100 partitions with a total mass of $N=100$ from a power law distribution (as is done in the ERW model of fragmentation [18]). After calculating χ_b^2 among them and averaging we obtained a value of 70% as our limit of confidence. In Fig. 6(a) we show the probability that the mass spectrum as a function of time and the asymptotic one come from the same distribution function for energy $E=-0.8\epsilon$, the circles represent the comparison with the ECRA result and the squares the comparison with MST spectra. The mass range which we used for this energy is $4\leqslant A\leqslant 60$. Figure 6(b) shows the same quantity but for energy $E=-0.3\epsilon$, in this case the mass range considered is $4\leqslant A\leqslant 24$. It can be seen from the figures above that at time $70t_0$ the ECRA result for energy $E=-0.8\epsilon$ is already very similar to the asymptotic value while the MST result bares little similarity. The case is exactly the same for $E=-0.3\epsilon$ but for time $40t_0$. The mass range considered was chosen taking into account the following arguments: the smaller bins (one to four) are very sensible to the evaporation process in which we are not interested. On the other hand the bigger bins show great fluctuations due to the finite size of our system. That is why we excluded these two mass ranges for our analysis. This kind of study is not suitable for high energies because the mass spectrum is very narrow and then the mass range to be considered for the comparison via χ_b^2 is far too small. The results we have obtained are summarized in the following: the ECRA mass spectra reaches their asymptotic values at time $\sim 12t_0$ for energies $E\geqslant -0.15\epsilon$, this being the CTS τ_{ecra}. For $E=-0.3\epsilon$ the time related to cluster formation is $\sim 40t_0$ and for $E=-0.8\epsilon$ the time is $\sim 70t_0$. This is a very important result because from it one can infer the kind of information contained in the asymptotic spectrum, i.e., the

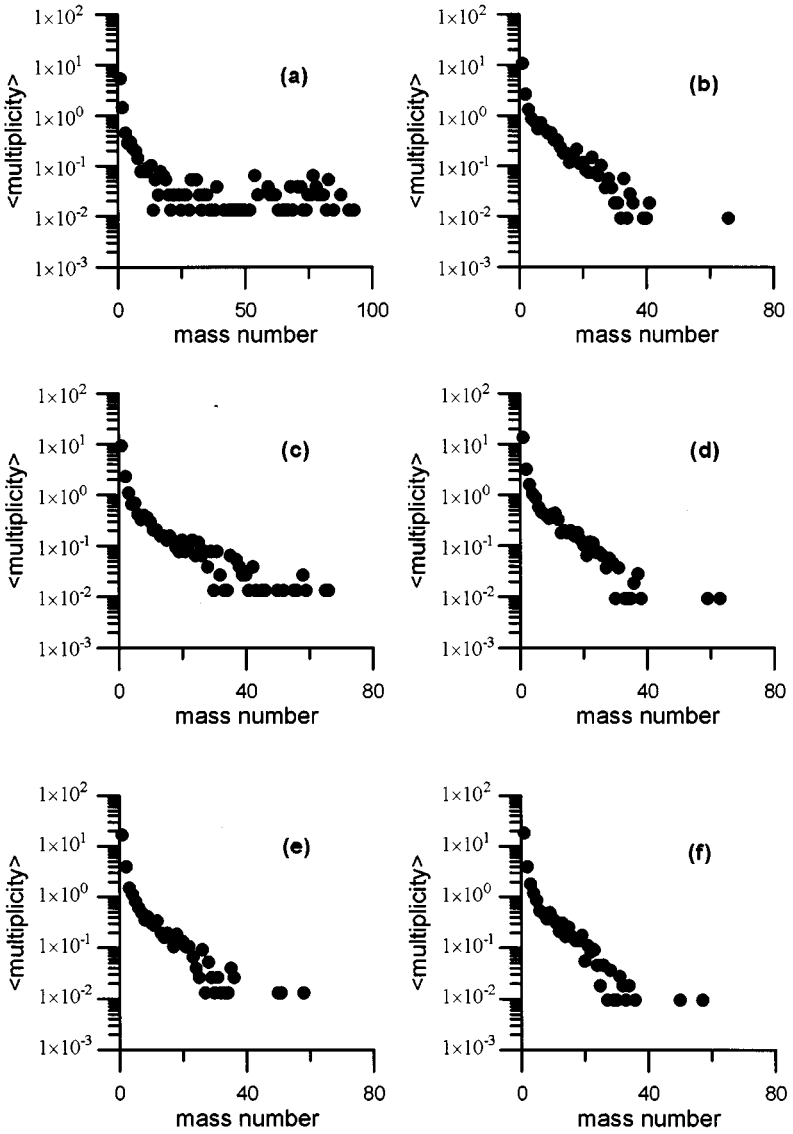

FIG. 3. Mass spectra for energy $E=-0.3\epsilon$, (a) MST result for time $40t_0$, (b) ECRA result for time $40t_0$, (c) MST result for time $80t_0$, (d) ECRA result for time $80t_0$, (e) MST result for time $200t_0$, and (f) ECRA result for time $200t_0$.

one obtained experimentally. In this way τ_{ecra} is the time after which the statistical properties of the mass distribution achieve their final values, so any information which the mass spectrum may carry concerns this initial stage ($t \leqslant \tau_{\mathrm{ecra}}$) of the process of multifragmentation in which the system is still dense and a MST analysis gives no information. In the following section we shall characterize this stage with respect to its velocity distribution.

Another way of studying the time properties of the MBDF spectra is by analyzing its shape as a function of time. According to Fisher's semiphenomenological droplet model for equilibrium liquid-gas transitions, the fragment mass distribution should be a power law multiplied by an exponential whose argument goes to zero at the critical point:

$$Y(A)=Y_0A^{-\tau}\exp\left[\frac{\mu_g-\mu_l}{T}A-\frac{4\pi r_0^2\sigma}{T}A^{2/3}\right],$$

where A is the mass of the drop, μ_g and μ_l are the chemical potentials of the bulk gas and liquid phases, and σ is the surface tension. This equation can be cast in the form

$$Y(A)=Y_0A^{-\tau}X^{A^{2/3}}Y^A, \tag{1}$$

where X and Y are fitting parameters (see [19] for details). At the critical point $\mu_g=\mu_l$ and therefore σ goes to zero, and we are left with a simple power law, which has the crucial property of being scale invariant. Fisher's scaling relation is common to other systems like percolation model, Ising model, etc. So if a given mass range of the spectrum is fitted with a power law $Y(A)\propto A^{-\tau}$, the exponent τ should be a minimum at the critical point. The mass range should be selected in such a way that (i) small fragments are left out because the scaling is supposed to be valid for not too small clusters [20], moreover, the population of the first bins is constantly increasing due to evaporation process and (ii) bigger clusters should be left out because either we are in the region of U shaped spectra in which case the effect of expo-

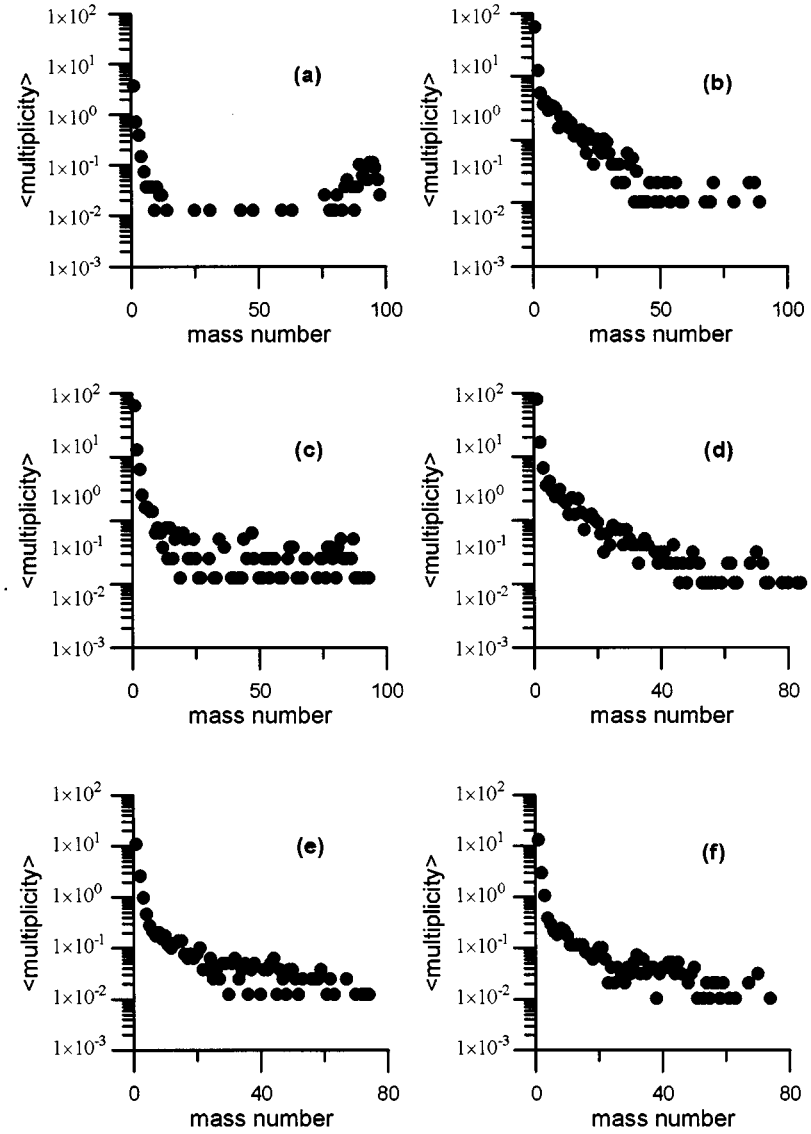

FIG. 4. Mass spectra for energy $E=-0.8\epsilon$, (a) MST result for time $40t_0$, (b) ECRA result for time $40t_0$, (c) MST result for time $80t_0$, (d) ECRA result for time $80t_0$, (e) MST result for time $200t_0$, and (f) ECRA result for time $200t_0$.

nential terms in the yield $Y(A)$ is strong or we are in the case of close to power law behavior for which we expect some sort of critical phenomena and the population of large mass bins is expected to fluctuate noticeably. Taking into account these considerations, in Fig. 7 we show the exponent τ as a function of the energy of the system, obtained by fitting the mass spectrum in the mass range $4\leqslant A\leqslant 20$ for all energies but for $E=-1\epsilon$ for which we took the range $4\leqslant A\leqslant 10$. This is because the plateau of the typical U shaped spectrum for $E=-1\epsilon$ a begins at mass number 10. It can be seen that minimum τ is achieved for $E=-0.8\epsilon$; nevertheless this result depends strongly on the mass range considered. To overcome this ambiguity we decided to study the dependence of the exponent τ with the mass range considered. In Fig. 8(a) we show τ as a function of time for energy $E=-0.8\epsilon$ for three mass ranges, namely $4\leqslant A\leqslant 20$ (circles), $4\leqslant A\leqslant 30$ (diamonds), and $4\leqslant A\leqslant 50$ (squares), it can be seen that the spectrum shows power law behavior and time invariance for time $\sim 70t_0$ onward. In Fig. 8(b) we show the exponent τ for $E=-0.55\epsilon$, in this case the spectrum is not a power law at any time (note the important dependence of the exponent on the mass range) but for time $\sim 60t_0$ onward the spectrum is quite invariant. A very similar result to this last one is obtained for energy $E=-0.3\epsilon$. The times involved in the asymptotization of the exponents is in agreement with the one obtained with the χ_b^2 test.

As stated in the Introduction, power law behavior in the mass distribution, for energy $E=-0.8\epsilon$, should not be related to Fisher's result for the critical point which applies for equilibrium systems. Nevertheless minimum τ and power law behavior in mass distribution, and consequently invariance against scale changes, can be the result of a critical process of some other kind. In any case the critical process takes place during the early stage of the process. It is worth mentioning at this point that according to the theory of critical phenomena the exponent τ should be greater than 2. The discrepancy of our result with this fact can be due to finite size effects, the decrease of τ with decreasing system size is

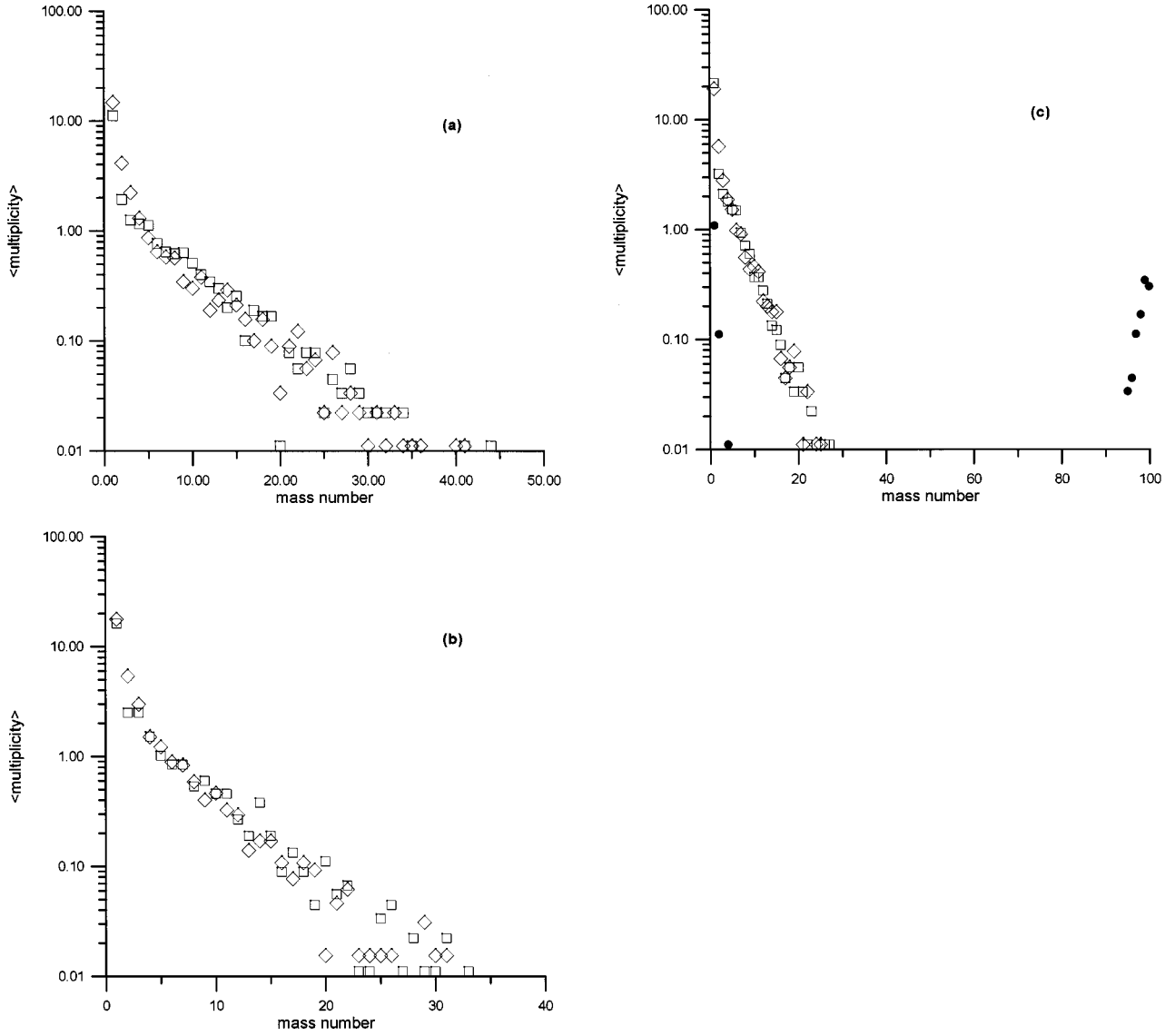

FIG. 5. (a) Mass spectra for energy $E=-0.15\epsilon$, ECRA result for time $10t_0$ (squares), and ECRA result for asymptotic time (diamonds). (b) Mass spectra for energy $E=0.3\epsilon$, ECRA result for time $10t_0$ (squares), and ECRA result for asymptotic time (diamonds). (c) Mass spectra for energy $E=0.8\epsilon$, ECRA result for time $10t_0$ (squares), MST result for time $10t_0$ (circles), and ECRA result for asymptotic time (diamonds).

well known in percolation calculations.

IV. COLLECTIVE EXPANSION AND TEMPERATURE

After showing that the statistical properties of the mass spectrum are stable after a short period of time, we explore the time evolution of two other relevant quantities defined in Sec. II, namely the mean radial velocity and the effective temperature of the expanding system.

In Fig. 9 we show the mean radial velocity (defined in Sec. II) of regions 2, 4, 6, and 8 as a function of time, for six different energies namely $E=1.8\epsilon$, 0.8ϵ, 0.3ϵ, -0.15ϵ, -0.3ϵ, and -0.8ϵ, averaged over approximately 100 evolutions each. We also show in Fig. 9 the collision rate for each energy (full thick line). The collision rate attains its asymptotic value at time $\sim 12t_0$ for all the energies considered. The first stage of the process ($t \leqslant 12t_0$) is a highly collisional one in which most of the radial flux is developed. Note that for energies greater than -0.3ϵ the radial velocity is almost completely developed at time $12t_0$ regardless of its energy. For energy $E=-0.3\epsilon$ the overall behavior is similar but the radial velocity goes on growing, at a smaller rate, after that time, and it reaches its asymptotic value at time $\sim 40t_0$. And for $E=-0.8\epsilon$ a very small radial flux is created but for some regions (regions 2 and 4) it starts to diminish after a short period of time and it reaches its asymptotic value at time $\sim 70t_0$. It is clear from Fig. 9 the role played by collisions in the radial flux formation. Interparticle collisions are responsible of transforming the initial thermal motion of constituent particles into the more ordered collective expansion. The dotted lines of Fig. 10 show the value of the potential energy per particle (scales are on the right Y axis) as a function of time for the above mentioned energies. We can see that by the time the collision frequency has reached the plateau, the potential energy reaches its maximum value, bringing into evidence that interactions between different clusters are neg-

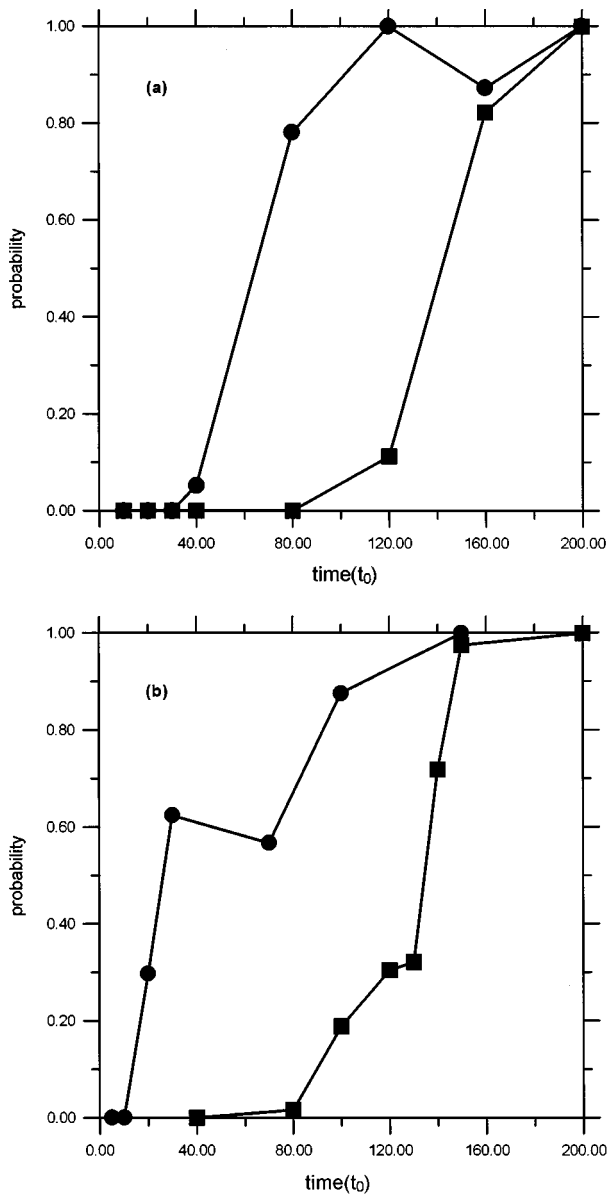

FIG. 6. Probability that the mass spectra at a given time and the asymptotic one come from the same distribution function for $E=-0.8\epsilon$ (a) and $E=-0.3\epsilon$ (b). The calculations are based on the χ_b^2 method. Circles denote ECRA spectra while squares refer to MST spectra.

ligible (although not zero, as can be seen from the MST analysis). As a consequence at this stage entropy production essentially stops.

In Fig. 10 we also show the ''temperature'' (as defined above) of the circular sectors as a function of time. The figures are characterized by a fast cooling down during the initial, highly collisional, stage of the evolution and afterwards they stabilize. Note that there is only a weak dependence of the ''temperature'' on the circular sector considered; furthermore, for times around $12t_0$ they are remarkably similar. Also note that before and after this period of time the temperature decreases as we move from the center of the system towards the outer regions and that the relative departures increase with time. A possible explanation of this facts will be given in the next section.

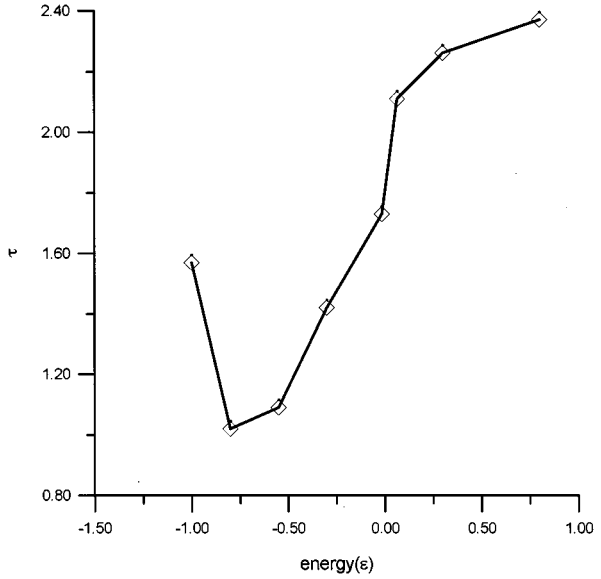

FIG. 7. Exponent τ as a function of energy (in units of ϵ). For all energies but $E=-1\epsilon$ the mass range considered in the fitting was $4\leqslant A\leqslant 20$, for $E=-1\epsilon$ it was $4\leqslant A\leqslant 10$.

Taking into account Figs. 5 and 9 it can be seen that, for energies $E\geqslant -0.15\epsilon$, by the time the radial flux attains its asymptotic value the MBDF become stable and the final mass distribution is obtained by the ECRA algorithm, i.e., the $\tau_{\rm flux}$ and $\tau_{\rm ecra}$ are very similar. This time ($12t_0$) coincides with the end of the initial collisional stage. For energy $E=-0.3\epsilon$ the system requires more time for the radial flux to achieve its asymptotic value (remember that the radial flux goes on growing for a while after the highly collisional stage has ended). The mass distribution, according to the ECRA algorithm, becomes stable at the same time ($t=40t_0$). For energy $E=-0.8\epsilon$ the case is similar to the last one, but the time required by the radial flux and by the mass spectra to become stable is a little longer ($\sim 70t_0$).

From the analysis of the data presented in the previous sections it is rather straightforward to realize that $\tau_{\rm coll}$ ($\sim 12t_0$) is quite independent of the energy and that at the end of this stage the ''temperature'' has reached its asymptotic value.

It can be seen that for energies $E\geqslant -0.15\epsilon$, for which the mass spectrum shape is of the exponential type, the radial flux and mass spectra are also stable at that time, so the following relation between the relevant time scales holds:

$$\tau_{\rm coll}\sim\tau_{\rm temp}\sim\tau_{\rm ecra}\sim\tau_{\rm flux}<\tau_{\rm mst}\,.$$

On the other hand, for the lower energies, when the mass spectrum shape becomes closer to a power law ($E=-0.3\epsilon$, -0.55ϵ and -0.8ϵ), we find that when the collision rate and ''temperature'' attain their plateau the radial flux is not completely developed (although its following time evolution takes place at a much lower rate). By the time the radial flux attains its final value the asymptotic fragments are detectable by the ECRA algorithm, so the following relation holds:

$$\tau_{\rm coll}\sim\tau_{\rm temp}<\tau_{\rm ecra}\sim\tau_{\rm flux}<\tau_{\rm mst}\,.$$

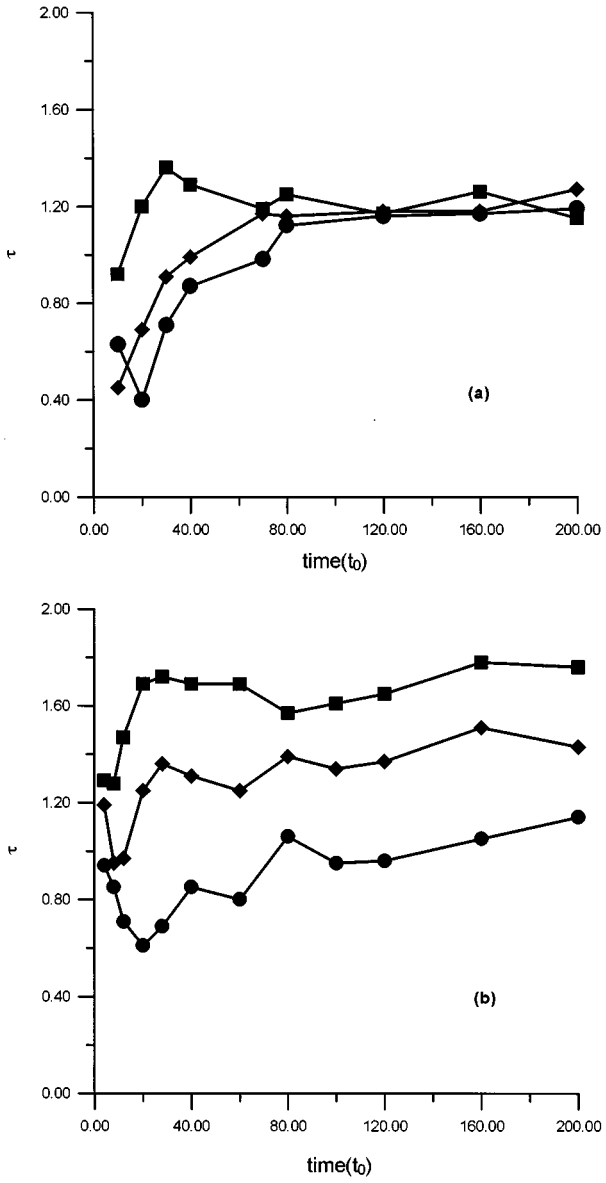

FIG. 8. Exponent τ as function of time for $E=-0.8\epsilon$ (a) and for $E=-0.5\epsilon$ (b) for three mass ranges: $4\leqslant A\leqslant 20$ (circles), $4\leqslant A\leqslant 30$ (diamonds), and $4\leqslant A\leqslant 50$ (squares).

V. THE EARLY CLUSTER FORMATION MODEL

From the results presented in the last two sections it is clear that, according to the excitation energy, multifragmentation can take place in two distinct ways: (a) expansion driven processes and (b) evaporation like processes. Most of the results presented correspond to events in the first regime, in which collisions generate a collective expansion, and it is this expansion the main ingredient determining the instability of the system against some density fluctuations, keeping in mind the close relation between flux formation and the stabilization of the mass spectra according to the ECRA model. In the second regime ($E<-0.8\epsilon$), the system expands during the early stages of its evolution and then the attractive part of the interaction makes the system contract after evaporating the outer particles. It is interesting to note that broadest mass distribution (minimum τ) and power law behavior of mass distribution was found, as in [21], for the events which lie in the transition from the expansion driven regime to the evaporation driven one.

The expansion driven multifragmentation processes present three distinct stages of evolution. The first stage is dominated by interparticle collisions and most part of the collective expansion builds up during it. The time involved in this stage is, for our system, $\sim 12t_0$. Once the collisional stage is over the system breaks up, at least when analyzed according to ECRA formalism. This is the second stage of the process. The time involved in this stage depends on the energy of the system, it is very short for the higher energies ($E\geqslant -0.15\epsilon$). For energy $E=-0.3\epsilon$ this second stage ends at time $t\sim 40t_0$ and for $E=-0.8\epsilon$ at $t\sim 70t_0$ (cf. Fig. 6). During the second stage the system is still dense and, regarding its velocity distribution, its state can be characterized by an almost homogeneous ''temperature'' (see Fig. 10) and by an expansion degree of freedom. Under these conditions, i.e., in the presence of a collective expansion and an almost uniform ''temperature,'' the MBDF develop and become stable, that is, the system breaks up. It is worth mentioning at this point that the MST cluster analysis during this stage gives no information about the asymptotic behavior of the system; in fact this kind of analysis gives longer times for cluster formation. In this way one would miss the relation between the formation of radial flux, ''temperature'' stabilization, and the appearance of the asymptotic clusters. The third stage is a very simple one, in which the system simply expands and the MBDF already formed spread in space and became separated drops. In this last stage the fragments keep on evaporating some particles but the multifragmentation process has finished.

In order to investigate the times at which the transition from multifragmentation to evaporation takes place we find it convenient to use the coefficient of persistence [22] defined by the following argument. Let $n_1 \ldots n_N$ the nucleons which belong to the cluster C with mass A_C at the time t. $b_C(t)=0.5{*}n_N(n_N-1)$ is then the number of pairs of nucleons in cluster C at that time. At the time Δt later, some of the nucleons may have left the cluster and belong to another cluster or be single particles. Let $N_{C\to A}$ be the number of nucleons which have been in the cluster C at time t and are at $t+\Delta t$ in the cluster A. We define $a_C(t+\Delta t)=\Sigma_A 0.5{*}[N_{C\to A}(N_{C\to A}-1)]$.

Now we are able to introduce the mass weighted persistence coefficient (P_m)

$$P_m(t)=\left\langle \left\langle \frac{a_C(t+\Delta t)}{b_C(t)}A_C \right\rangle_{\rm cl} \right\rangle_e ,$$

where $\langle\rangle_{\rm cl}$ denotes average over the clusters at time t and $\langle\rangle_e$ denotes average over the ensemble of explosions at a given energy. $P_m(t)$ will be equal to 1 if all particles remain together and 0 if the clusters break up completely. It measures the tendency of the members of a given cluster to remain together. We next show the persistence coefficient as a function of time (circles of Fig. 11) for energies $E=-0.8\epsilon$ [Fig. 11(a)], -0.55ϵ [Fig. 11(b)], and -0.3ϵ [Fig. 11(c)], together with the value of the mass weighted persistence related to evaporation, $P_m^{(-1)}(t)$, which is calculated from the fragment configurations at time t by considering that all frag-

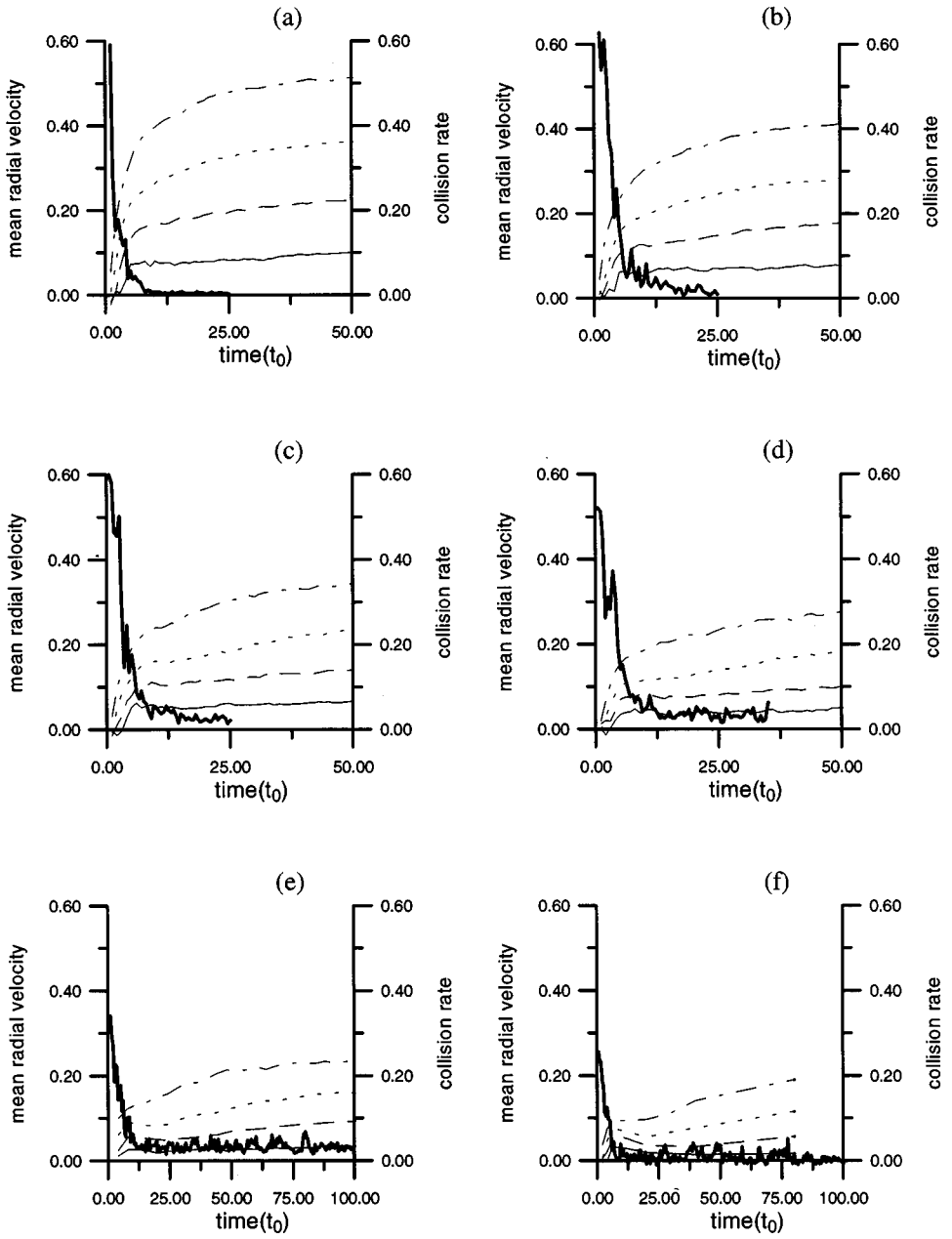

FIG. 9. Collision rate in arbitrary units (full thick lines) and mean radial velocity (in units of σ/t_0) as a function of time (in units of t_0) of regions 2 (full thin lines), 4 (dotted lines), 6 (dashed lines), and 8 (dashed-dotted lines). For energies: (a) $E=1.8\epsilon$, (b) $E=0.8\epsilon$, (c) $E=0.3\epsilon$, (d) $E=-0.015\epsilon$, (e) $E=-0.3\epsilon$, and (f) $E=-0.8\epsilon$.

ments with mass bigger than 4 lose one particle (triangles of Fig. 11). For these calculations we took $\Delta t=5t_0$ for energy $E=-0.3\epsilon$, $\Delta t=4t_0$ for energy $E=-0.55\epsilon$, and $\Delta t=10t_0$ for energy $E=-0.8\epsilon$. It can be seen that, after the initial stage of the process the main decay channel for the medium mass fragments is evaporation. The time at which the multifragmentation stage ends and we are left with evaporation is $\sim 40t_0$ for energy $E=-0.3\epsilon$, $\sim 60t_0$ for energy $E=-0.55\epsilon$, and $\sim 100t_0$ for energy $E=-0.8\epsilon$. This result is consistent with the ones presented in Secs. III and IV.

Because at this times the systems are still dense according to MST recognition algorithm, the study of the above defined persistence coefficient states that the MBDF (recognized by the ECRA algorithm) have reached microscopic stability.

Regarding the temperature evolution in time note that during the first stage of the evolution ($t<10t_0$) the outer regions cool down more rapidly than the central ones, this is because the expansion starts to develop in the outer region, so ''temperature'' in this regions is converted into expansion more quickly. An important question at this point regards whether the homogenization of the temperature at time $\sim 10t_0$ is the result of thermalization or not. Lets analyze the velocity fluctuations over the expansion (which are related to the temperature) at times shorter than $10t_0$, lets take some characteristic temperature of this early stage of the evolution, say $T=1\epsilon$, the mean velocity associated with it is approximately $0.2\sigma/t_0$. Lets also consider some characteristic variation of mean radial velocity between adjacent circular regions,

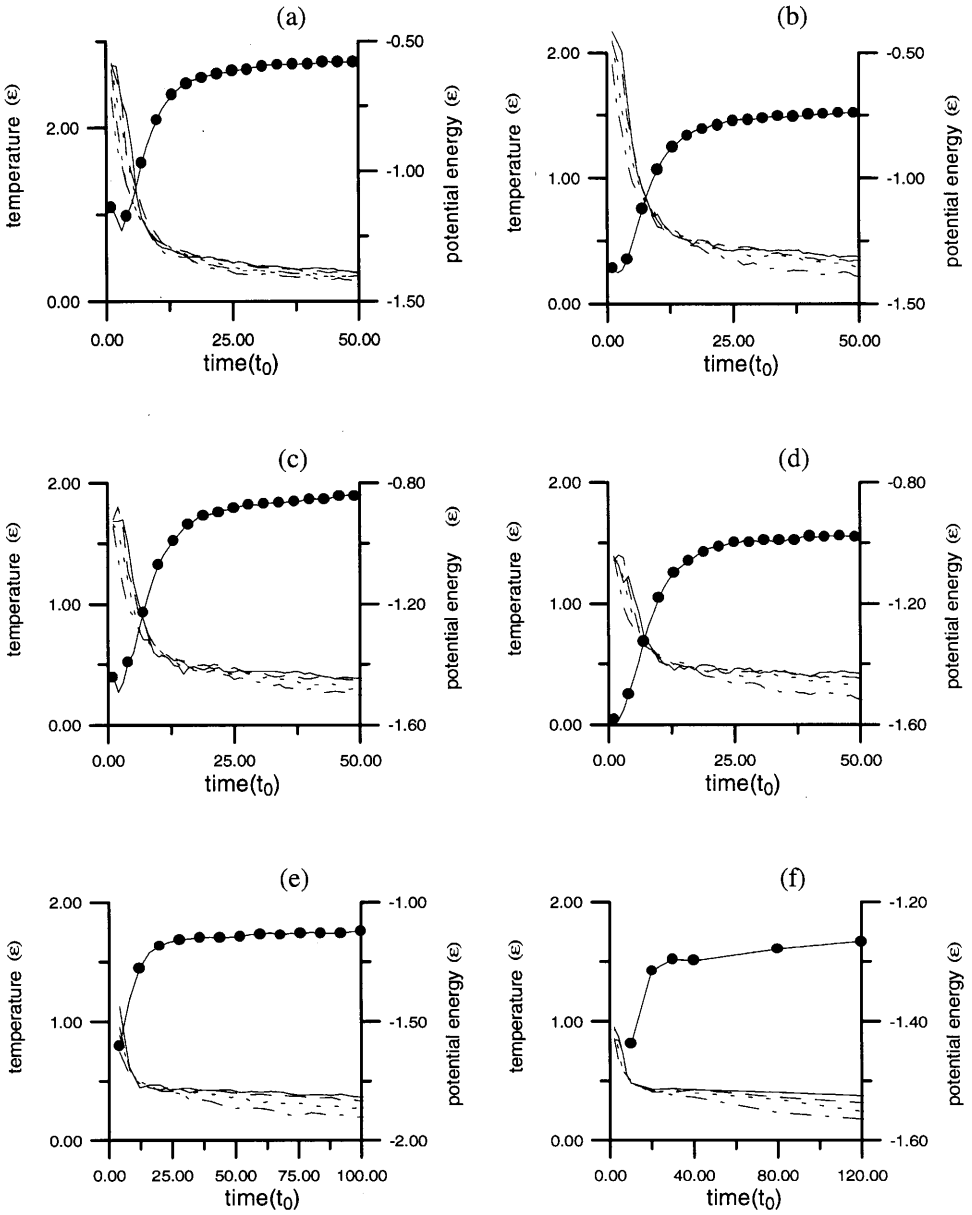

FIG. 10. Potential energy per particle, in units of ϵ (dotted lines) on the right Y axis and, on the left Y axis, temperature, in units of ϵ, of regions 2 (full thin lines), 4 (dotted lines), 6 (dashed lines) and 8 (dashed-dotted lines) as a function of time (in units of t_0). For energies: (a) $E=1.8\epsilon$, (b) $E=0.8\epsilon$, (c) $E=0.3\epsilon$, (d) $E=-0.015\epsilon$, (e) $E=-0.3\epsilon$, and (f) $E=-0.8\epsilon$.

$\Delta v_{\mathrm{rad}} \simeq 0.05\sigma/t_0$. This means that during a lapse of time of $10t_0$ two adjacent regions move $\sim 0.5\sigma$ away from each other while the mean distance traveled by a particle over the expansion is $\sim 2\sigma$, it is possible, then, that during a time of $10t_0$ local thermal equilibrium be achieved. From Fig. 10 it can be seen that during the breakup, i.e., the second stage of the process, the ''temperature'' of the system is quite homogenous. It can also be seen from Fig. 10 that, once the second stage is over, the inner regions are hotter than the outer ones, for all the energies which we studied. This fact is also explained by our multifragmentation model as can be seen by the following argument. We studied the correlation between cluster size and relative position of its center of mass (c.m.) in the system; in Fig. 12 we show the mean distance from the c.m. of the system to the c.m. of the asymptotic fragments as a function of the mass of the clusters for $E=-0.15\epsilon$. It is seen that the heavier fragments appear near the c.m. of the system, as we move away from it lighter fragments appear. This behavior is also seen for all the other energies analyzed in this work. Remember that according to our multifragmentation model the breakup state is characterized by a local mean radial velocity and by an almost homogeneous ''temperature,'' so, due to the expansion, the kinetic energy of a cluster, measured from its c.m., increases with its size. As the clusters move away from each other, the expansive kinetic energy is converted back into ''temperature.'' In this way the bigger clusters will be hotter than the smaller ones; taking into account Fig. 12, the central regions will be hotter than the outer ones.

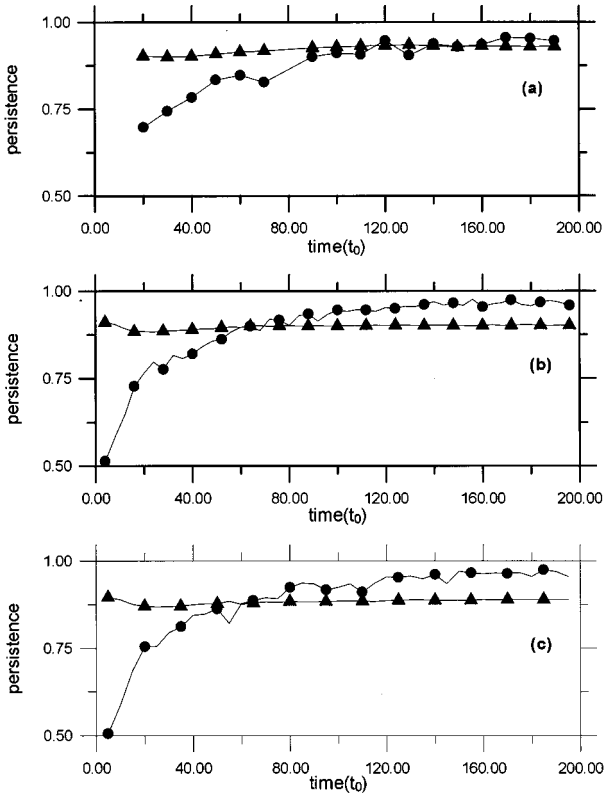

FIG. 11. Persistence coefficient as a function of time $P_m(t)$ (circles) and reference evaporation persistence value $P_m^{(-1)}(t)$ (triangles). (a) Energy: $E=-0.8\epsilon$, (b) $E=-0.55\epsilon$, and (c) $E=-0.3\epsilon$.

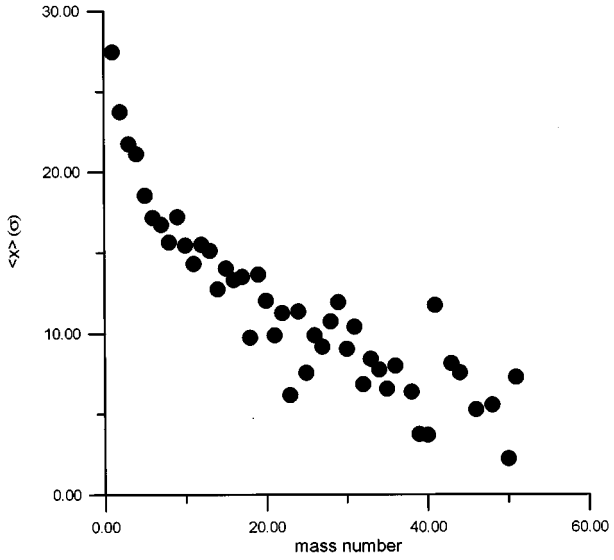

FIG. 12. Mean position of the asymptotic clusters (in units of σ) as a function of its mass number for energy $E=-0.15\epsilon$.

VI. CONCLUSIONS

In this work we have studied the relation between fragment formation, local ''thermal'' equilibration, and stabilization of the statistical properties of the mass spectrum. We found, as in previous calculations, that the asymptotic fragments, in fact the density fluctuations which lead to the asymptotic fragments, are formed early in the evolution of the expanding drops, when the system is still dense. This result had already suggested that the information contained in the asymptotic mass spectrum corresponded to these early stages of the evolution. We have advanced in this respect by showing the novel result that the overall statistical properties of the cluster spectrum are equivalent to the asymptotic ones after a short time τ_{ecra}. Furthermore, we were able to characterize this breakup state as regards its velocity distribution. We found that at the time of effective breakup, when the MBDF form, the state of the system can be characterized by an almost uniform ''temperature'' over a local mean radial velocity which is an increasing function of the distance from the center of mass of the system. So the conclusions which one can obtained by studying mass spectra concerns this state. The mean radial velocity gradient depends on the total energy of the system while the asymptotic ''temperature'' is quite independent of it. As a by-product these results might provide a basis for a microscopic foundation of, properly modified, thermodynamic models.

We also found that for a short initial time the system undergoes a highly collisional stage which is responsible for the creation of the radial flux, once this early stage ends, the ''temperature'' of the system has reached its asymptotic value.

We found power law behavior in the mass spectra for energies around $E=-0.8\epsilon$ and we would like to recall once again that this result cannot be directly related to Fisher's result of liquid-gas equilibrium transition at the critical point, because our system is fragmenting in the presence of a collective expansion.

ACKNOWLEDGMENTS

Partial financial support via Grant No. EX-076, University of Buenos Aires, is acknowledged.

[1] F. Sebille *et al.*, Nucl. Phys. **A501**, 137 (1989).
[2] G. F. Berstch and S. das Gupta, Phys. Rep. **160**, 190 (1988).
[3] D. H. E. Gross, Rep. Prog. Phys. **53**, 605 (1990).
[4] D. H. E. Gross, Ref. [3]; J. P. Bondorf, A. S. Botvina, A. S. Iljinov, I. N. Mishustin, and K. Sneppen, Phys. Rep. **257**, 133 (1995).
[5] J. Randrup and S. E. Koonin, Nucl. Phys. **A356**, 223 (1981).
[6] R. J. Lenk, T. J. Schlagl, and V. R. Pandharipande, Phys. Rev. C **42**, 372 (1990).
[7] C. O. Dorso and J. Randrup, Phys. Lett. B **215**, 611 (1988).
[8] J. Aichelin, Phys. Rep. **5&6**, 233 (1991).
[9] C. O. Dorso and J. Randrup, Phys. Lett. B **301**, 328 (1993).
[10] C. O. Dorso and P. Balonga, Phys. Rev. C **50**, 991 (1994).
[11] C. O. Dorso and P. Balonga, Phys. Lett. B **345**, 197 (1995).

[12] C. O. Dorso and A. Strachan, Phys. Rev. B **50**, 236 (1996).
[13] M. E. Fisher, Physics (Long Island City, NY) **3**, 255 (1967); Rep. Prog. Phys. **30**, 615 (1967).
[14] A. Vicentini, G. Jacucci, and V. R. Pandaharipande, Phys. Rev. C **31**, 1783 (1985).
[15] F. F. Abraham, Adv. Phys. **35**, 1 (1986).
[16] C. O. Dorso and J. Randrup, Phys. Lett. B **232**, 29 (1989).
[17] W. H. Press, B. P. Flannery, S. A. Teukolsky, and W. T.Vetterling, *Numerical Recipes, The Art of Scientific Computing*-(Cambridge University Press, Cambridge, England, 1986).
[18] B. Ellatari, J. Richert, and P. Wagner, Phys. Rev. Lett. **69**, 45 (1992); Nucl. Phys. **A560**, 603 (1993).
[19] V. Latora, M. Belkacem, and A. Bonasera, Phys. Rev. Lett. **73**, 1765 (1994).
[20] D. Stauffer, *Introduction to Percolation Theory* (Taylor & Francis, London 1985).
[21] S. Pratt, C. Montoya, and F. Ronning, Phys. Lett. B **349**, 261 (1995).
[22] C. O. Dorso and J. Aichelin, Phys. Lett. B **345**, 197 (1995).